

WELDING SIMULATION OF TEMPERATURE DISTRIBUTION OF BUTT WELDED PLATES USING GTAW

Hitesh Arora^{a1}, Mandeep Singh Rayat^{a4}

hitesh.15774@lpu.co.in

mandeep.16445@lpu.co.in

^aAssistant Professor, Lovely Professional University, Punjab, India

ABSTRACT

Tungsten inert gas (TIG) welding, also known as Gas tungsten arc welding (GTAW), is a arc welding process that uses a non-consumable tungsten terminal to deliver the weld. The weld zone and anode is shielded from oxidation or other air defilement by an idle protecting gas (argon or helium), and a filler metal is typically utilized, however a few welds, known as autogenous welds, don't require it. A consistent current welding power supply produces electrical vitality, which is led over the curve through a segment of exceptionally ionized gas and metal vapors known as a plasma.

INTRODUCTION

TIG is most generally used to weld thin areas of stainless steel and non-ferrous metals, for example, aluminum, magnesium, and copper composites. The procedure gives the administrator more prominent control over the weld than contending procedures, for example, protected metal curve welding and gas metal circular segment welding, taking into consideration more grounded, higher quality welds. Be that as it may, GTAW is nearly more mind boggling and hard to ace, and moreover, it is altogether slower than most other welding procedures. A related procedure, plasma circular segment welding, utilizes a marginally unique welding light to make a more engaged welding bend and subsequently is frequently robotized.

REVIEW OF LITRATURE

In 1946 Rosenthal built up a connection for both line and point moving sources. In 1969 Pavelic presented Gaussian type of circulation which is utilized by numerous specialists and has been utilizing the same on account of its effortlessness and precision of such a presumption. Later John Goldack et al.[1] presented a twofold ellipsoidal warmth dissemination demonstrate. Sabapathy et al. [2] built up a changed twofold ellipsoidal warmth circulation show.

Ueda and Yamakawautilized[3] 2D limited component examination to ascertain the welding residual stresses for the first time. They broke down the impact of geometry setup on leftover anxiety and contrasted the outcomes and X-Ray diffraction strategy. Numerous others likewise proposed FEM models to foresee lingering stresses. R A Owen et al.[4] introduced a correlation among neutron diffraction; X-beam diffraction, synchrotron X-beam diffraction and Finite component demonstrate aftereffects of lingering stress

created amid welding of aluminum compound AA2024.

Senior member Dean Deng et al.[5].developed a 3D FE demonstrate for recreating lingering worries amid multipass welding of a pipe. The circulation of remaining worry in welded pipe structures relies upon a few factors, for example, auxiliary measurements, material properties, warm information, number of weld pass and welding grouping, and so forth.

Afzaal M. Malik et al. [6] dissected the leftover anxiety fields in circumferentially bend welded thin-walled chambers. So as to lessen the computational time and cost, a large portion of the specialists pick the axisymmetric models. Brickstad and Josefon[7] utilized 2D axisymmetric model to reenact circumferential welding of stainless steel speak up to 40 mm thick in a non-direct thermo-mechanical limited component investigation.

In the present examination, a three dimensional limited component demonstrate is created to mimic the temperature fields and leftover anxiety fields created amid welding of funnels. The model is approved utilizing the trial comes about introduced by Dean Deng et al.[8].

Sanjeev kumar et. al [9] attempted to explore the possibility for welding of higher thickness plates by TIG welding. Aluminium Plates (3-5mm thickness) were welded by Pulsed Tungsten Inert Gas Welding process with welding current in the range 48-112 A and

gas flowrate 7 -15 l/min. Shear strength of weld metal (73MPa) was found less than parent metal(85 MPa). From the analysis of photomicrograph of welded specimen it has been found that,weld deposits are form co-axial dendrite micro-structure towards the fusion line and tensile fracture occur near to fusion line of weld deposit.

Indira Rani et. al [10] investigated the mechanical properties of the weldments of AA6351 during the GTAW /TIG welding with non-pulsed and pulsed current at different frequencies. Welding was performed with current 70-74 A, arc travel speed 700-760 mm/min, and pulse frequency 3 and 7 Hz. From the experimental results it was concluded that the tensile strength and YS of the weldments is closer to base metal. Failure location of weldments occurred at HAZ and from this we said that weldments have better weld joint strength

Preston et.al [11] developed a finite element model to predict the evolution of residual stress and distortion dependence on the yield stress-temp for 3.2 mm 2024 Al alloy by TIG welding. Akbar Mousavi analysed the effect of geometry configurations on the residual stress distributions in TIG weld from predicted data and compared it with data obtained by XRay diffraction method. Attempts were made to analyse the residual stresses produced in the TIG welding process using 2D and 3D finite element analysis. For welding of 10 mm thick 304 grade stainless steel welding current in the range 80-225 A, voltage 15 V, and welding velocity in the range of 90-192 mm/min were employed.

Wang Rui et. al [12] investigated the effect of process parameters i.e. plate thickness, welding heat input on distortion of Al alloy 5A12 during TIG welding. For welding they used current (60-100) A, welding speed (800-1400) mm/min and thickness of w/p (2.5-6) mm. The results show that the plate thickness and welding heat input have great effect on the dynamic process and residual distortion of out-of-plane.

Finite element modeling

The finite element method (FEM) is a numerical strategy for tackling issues of designing and scientific material science. It is also referred to as finite element analysis (FEA). Typical problem areas of interest include structural analysis, heat exchange, liquid stream, mass transport, and electromagnetic potential. The expository arrangement of these issues for the most part require the answer for limit esteem issues for fractional differential conditions. The limited component technique definition of the issue brings about an arrangement of mathematical conditions. The technique yields inexact estimations of the questions at discrete number of focuses over the domain. To tackle the issue, it subdivides a vast issue into littler, less complex parts that are called limited components. The basic conditions that model these limited components are then gathered into a bigger arrangement of conditions that models the whole issue. FEM at that point utilizes variational strategies from the math of varieties to surmised an answer by limiting a related blunder work.

The analysis of welding forms includes a few branches of material science, and requires the coupling of various models routed to depict the phenomenological conduct of a framework. Huge numbers of these models have been actualized numerically and are being utilized as a part of a productive approach to take care of the issues on an individual premise.

In the arc welding process, the vitality required for metal combination is delivered by the Joule impact. This impact delivers the vitality required to soften the base and filler metals, framing what is known as the fluid pool. The surface temperature of the piece shifts from 1700 K to 2500 K, contingent upon the material. In the fluid pool, convective impacts happen that enhance the warmth transport. At long last, in the wake of expelling the warmth sources, the metal hardens.[5]

Experimentation

Weld bead

Weld bead is a deposit of filler metal from a single welding pass. A weld deposit resulting from a single longitudinal progression of a welding operation along joint.

A summary of the geometric characteristics of the weld bead obtained are presented in Table and shown in Figure.

Welding	width(mm)	depth(mm)	bead height(mm)
TIG	5.13	1.82	1.12

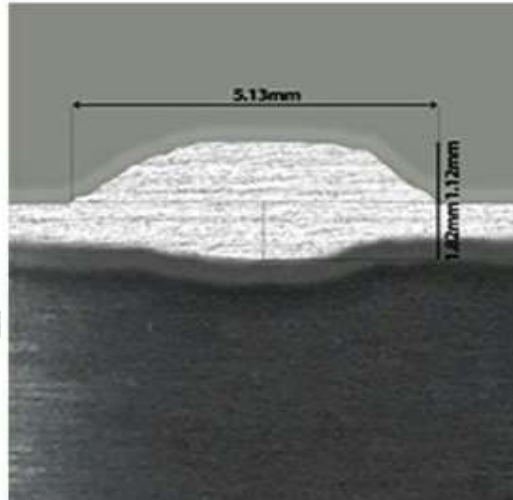


Figure 1: Weld bead size in mm

Analysis model

Welding residual stresses distributions are calculated by a finite element method. Theoretical considerations can be assessed either by a thermal or a mechanical model.

Thermal model

A control volume is bounded by an arbitrary surface; the fundamental equation of heat conduction is

$$\begin{aligned} \rho C \frac{\partial T}{\partial t} &= \{L\}^T ([D]) \{L\} T + Q \\ &= \frac{\partial}{\partial x} \left(k_x \frac{\partial T}{\partial x} \right) + \frac{\partial}{\partial y} \left(k_y \frac{\partial T}{\partial y} \right) + \frac{\partial}{\partial z} \left(k_z \frac{\partial T}{\partial z} \right) + Q \end{aligned}$$

and the boundary condition of heat convection over the control volume surface is

$$\{q\}^T \{\eta\} = -h_f (T_B - T_A)$$

where ρ is density, C is specific heat, T is temperature, t is time, q is heat flux, Q is the rate of internal heat generation, h is the unit outward normal vector, h_f is the film coefficient, T_B is the bulk temperature of the adjacent fluid, and T_A is the temperature the surface of the model. Pre multiplying the governing equation by a virtual change in temperature, integrating over the volume of the element and considering the boundary condition.[7]

Physical modeling

A plate with length 150 mm, thickness of 10 mm, and an aggregate width of 100 mm as appeared in fig.3 is considered for the examination. The material utilized is SS304 stainless steel. In this examination, two pass TIG welding with a between pass temperature of 50°C is utilized.

Thermal modeling

Examination is improved the situation of steel plate of length 150mm and thickness 10mm as appeared in Fig.1 Since the plate is symmetrical, half of the plate is just displayed. By utilizing proper work improvement strategy, generally fine work is produced in and around the weld lines and relatively coarse work is in ranges far from weld line as appeared in fig 1. 8 hub block warm component is utilized for the warm investigation. The administering condition for transient warmth exchange amid welding is given by

$$\rho c \frac{\partial y}{\partial x}(x, y, z, t) = -\nabla \cdot q(x, y, z, t) + Q(x, y, z, t)$$

Where p is the thickness of the materials, c is the particular warmth limit, T is the temperature, q is the warmth motion vector, Q is the inner warmth age rate, x , y and z are the directions in the reference framework, t is time and ∇ is the spatial slope administrator. To play out the investigation, the warmth dispersion demonstrate is adjusted keeping in mind the end goal to oblige tube shaped directions. The pipe geometry is produced and TIG welding light is connected along the boundary utilizing the welding parameters. Fig.2 demonstrates the different weld pool parameters, in a double ellipsoidal dissemination proposed by Goldak.

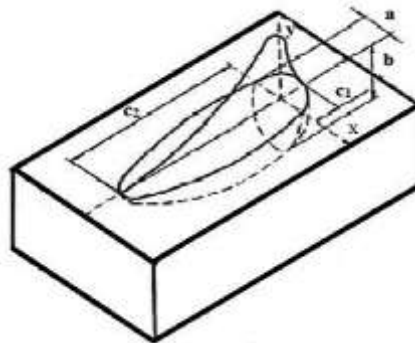


Figure 2: Double Ellipsoidal Heat Source

The parameters a , b , c_1 and c_2 are identified with the attributes of the welding heat source. The warmth source

Parameters are dictated by explaining observational relations accessible in writing of Dean Deng et al. In the present think about, the warmth from the moving welding curve is connected as a volumetric warmth source with a double ellipsoidal appropriation proposed by Goldak. and is communicated by the accompanying conditions:

$$Q(x, y, z, t) = \frac{6\sqrt{3}f_i\eta VI}{abc\pi\sqrt{\pi}} e^{\left[-3\left(\frac{x-vt}{c}\right)^2 - 3\left(\frac{y}{b}\right)^2 - 3\left(\frac{z}{a}\right)^2\right]}$$

where x, y and z are the nearby arrangements of the twofold ellipsoid model. f_i is the part of warmth saved in the weld area. V and I are the connected voltage and current separately. η is the curve productivity for the TIG welding process, v is the speed of light go in mm/s and t is the time in seconds. The parameters a, b and c are identified with the qualities of the welding heat source. The parameters of the warmth source are picked by the welding conditions.

To consider the warmth misfortunes, both the thermal radiation and convective heat exchange on the weld surface are accounted. Radiation misfortunes are overwhelming at higher temperature districts in and around the weld zone, and convection misfortunes are conspicuous at bring down temperatures far from the weld zone. Client subroutine was created and connected to mimic the consolidated convective and radiation limit conditions. The consolidated convective and radiative warmth exchange coefficient from Dean Deng

$$h = \{ 0.68T \times 10^{-8} (W/mm^2) \quad 0 < T < 500 \text{ }^\circ\text{C}$$

$$h = (0.231T - 82.1) \times 10^{-8} (W/mm^2) \quad T > 500 \text{ }^\circ\text{C}$$

where T is the temperature in $^\circ\text{C}$

So as to play out the warm examination the plate is demonstrated in tube shaped directions. At that point Goldak condition is changed to suit tube shaped organizes as underneath,

$$Q(x, y, z, t) = \frac{6\sqrt{3}f_i\eta}{abc\pi\sqrt{\pi}} \exp \left[-3 \left(\frac{r\theta - vt}{a} \right)^2 - 3 \left(\frac{z}{b} \right)^2 - 3 \left(\frac{r-R}{c} \right)^2 \right]$$

subroutine is produced utilizing to apply the warmth age to the plate. It is accepted that the pipe is welded along its periphery, and side inverse to weld line is thought to be settled, with a specific end goal to get quicker union amid numerical examination. The bend productivity is thought to be 70 %. The convective warm limit condition is utilized for every single free limit of the pipe. The warm impacts because of hardening of the weld pool are displayed by utilizing enthalpy strategy by bookkeeping idle weld.

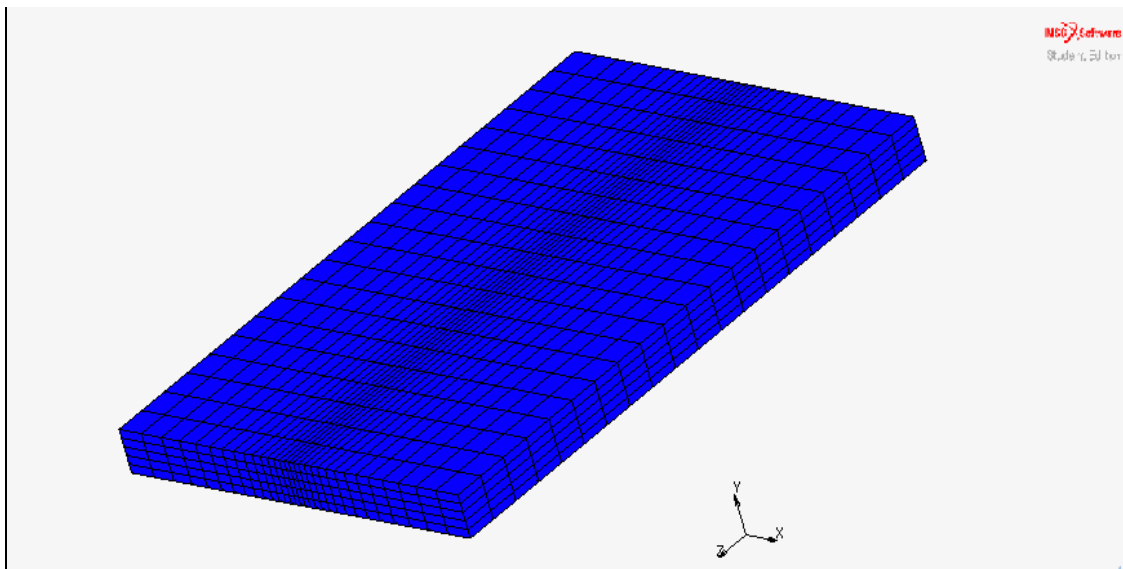


Figure 3 : Meshed model

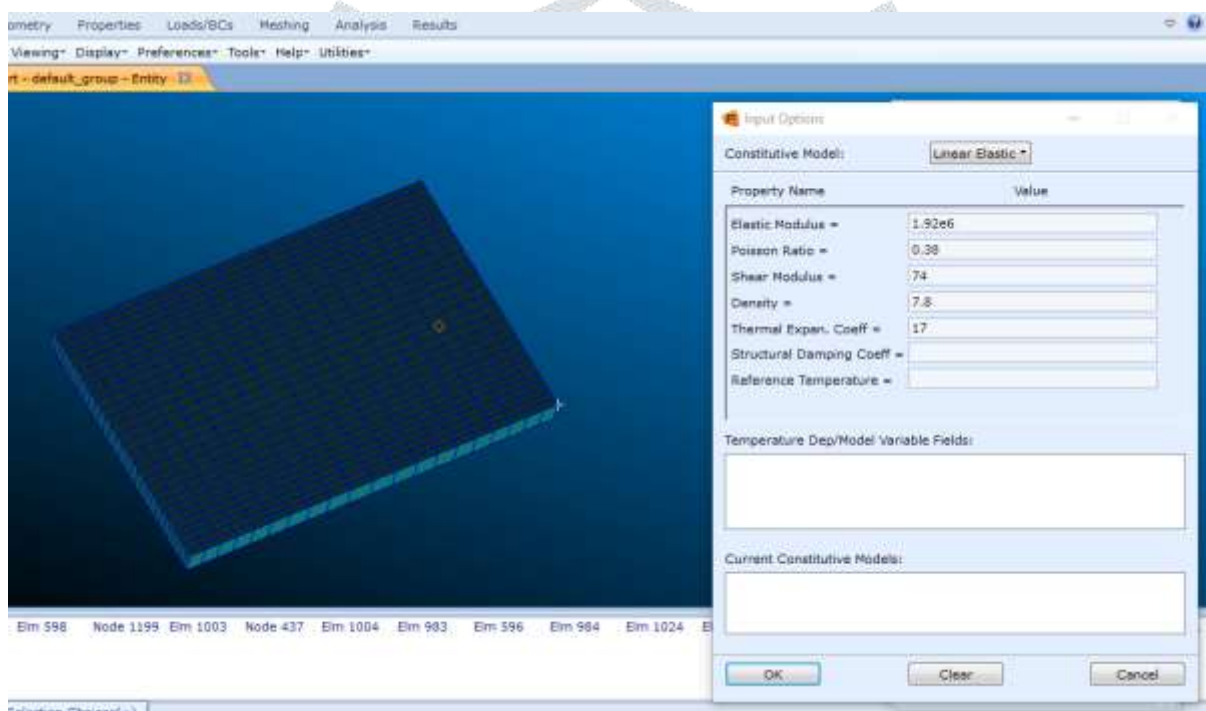


Figure 4 : Material properties

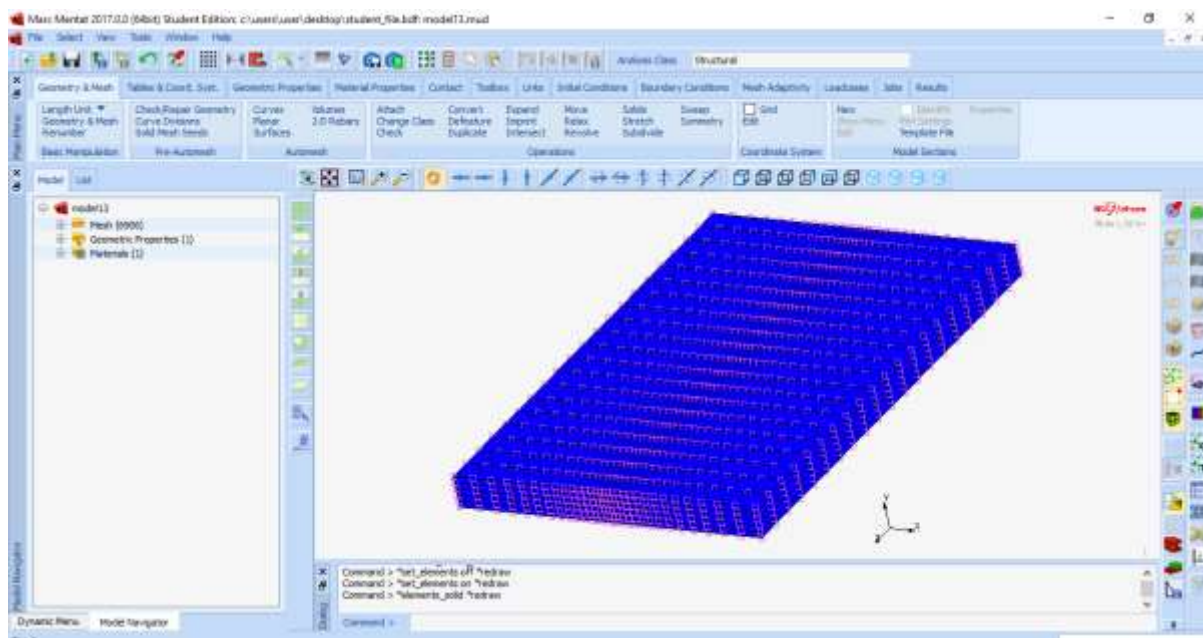


Figure 5: Marc Import

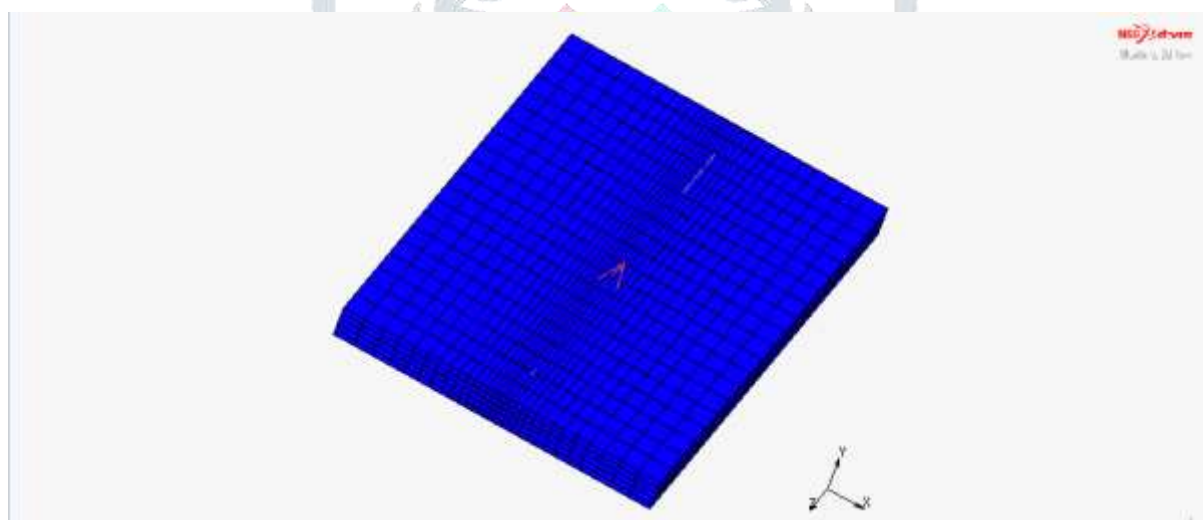


Figure 6 : Weld path

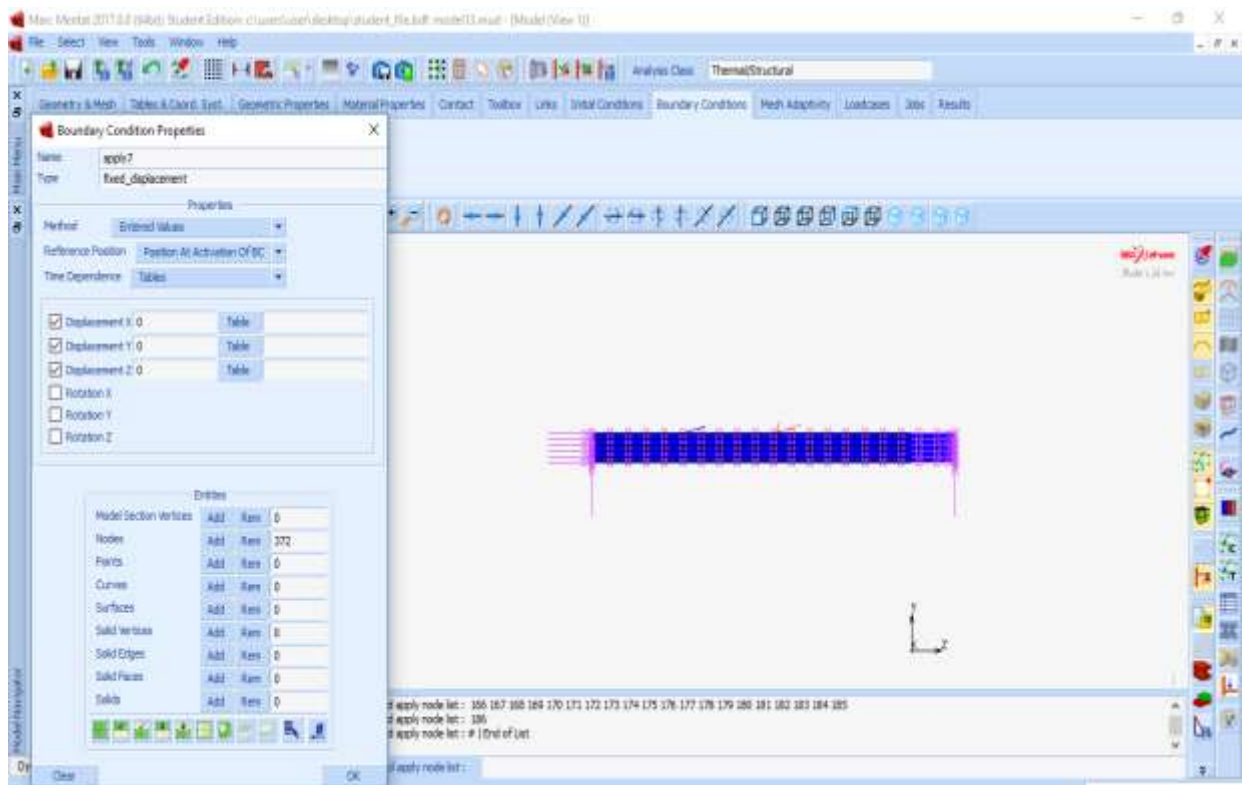
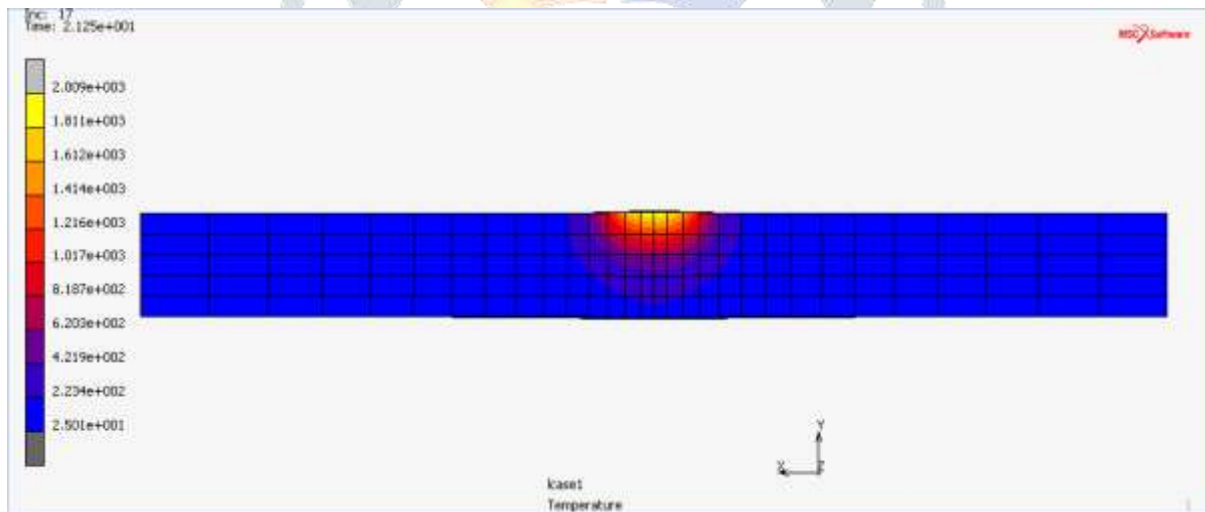
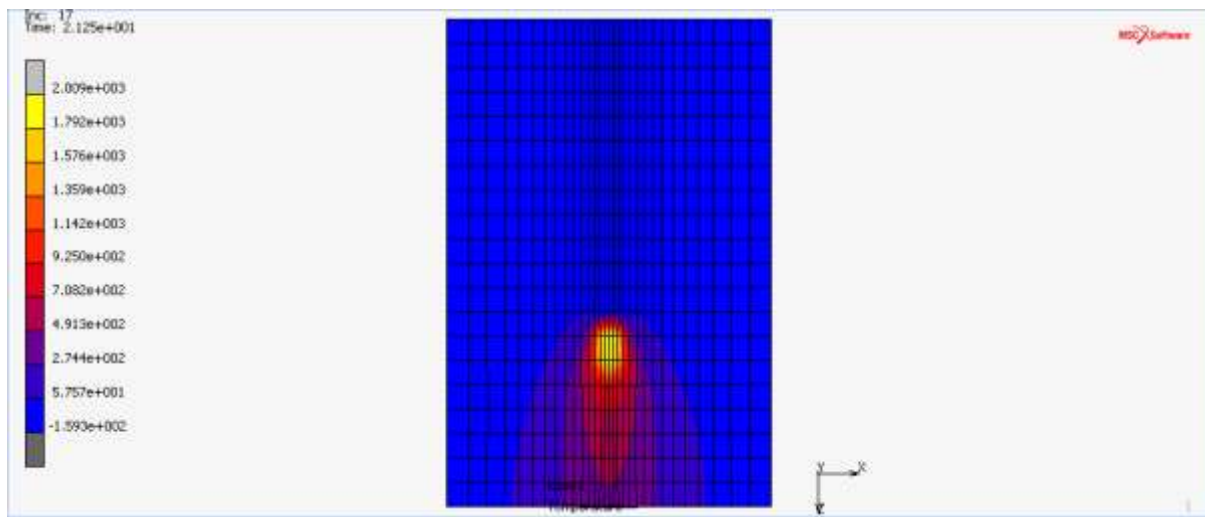


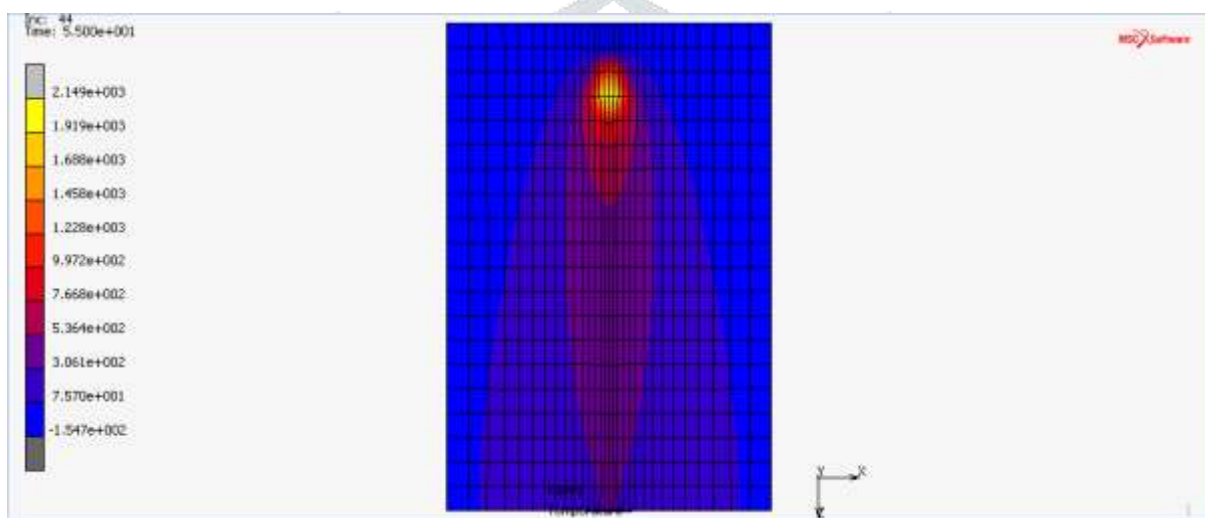
Figure 7 : Boundary conditions(thermal and structural)



(a)



(b)



(c)

Figure 8 (a-c) : Temperature profile

Conclusion-

- The weld bead profile is showing the microscopic image of the weld. Through the weld profile we get the exact size (width, depth and bead height) of the welding. The data we will get shows that the width of weld bead is 5.13mm, depth is 1.82 mm and height is 1.12 mm.
- The finite element method including the birth and death technique is an efficient methodology to investigate the vertical removal, development at various plate areas in the welding procedure of stainless steels, as well as their angular deformation and longitudinal bending.
- A technique for determining the double ellipsoid heat source parameters in the deposition of one weld bead for TIG was introduced. A right heat distribution was gotten, which is imperative for assist simulations including metallurgical and mechanical modeling.

- Compare the practical and experimental tests, the proposed methodology showed close results for the case study. The time consumed to determine the heat source pa-rameters is reduced when compared with the parameters determination by trial and error.

References

1. Weman, Klas (2003). Welding processes handbook pp. 31, 37–38
2. John Goldack, Aditya Chakravarti and Malcolm Bibby., A new finite element model for welding heat sources, J. Metallurgical Transactions B 15, 1984, p. 299-305.
3. D.Klobcar, J. Tusek B. Taljat, Finite element modeling of GTA weld surfacing applied to hot-work tooling, J. Comp. Mater. Sci. 31, 2004, p.368–378.
4. S.A.A. AkbariMousavi, R.Miresmaeili, Experimental and numerical analyses of residual stress distributions in TIG welding process for 304L stainless steel, J. Mater.Process. Technology 208, 2008, p. 383–394.
5. R.A. Owen, R.V Preston, P.J Withers, H.R Shercliff, P.J Webster, Neutron and synchrotron measurements of residual strain in TIG welded aluminium alloy 2024, Journal of Materials Science and Engineering: A, 346, 2003, p. 159-167.
6. Dean Deng, HidekazuMurakawa, Numerical simulation of temperature field and residual stress in multi-pass welds in stainless steel pipe and comparison with experimental measurements, Journal of Computational Materials Science 37, 2006, p. 269 – 277.
7. AfzaalM. Malik, Ejaz M. Qureshi, Naeem Ullah Dar, Iqbal Khan, Analysis of circumferentially arc welded thin-walled cylinders to investigate the residual stress fields, J. Thin-Walled Structures-46, 2008, p. 1391– 1401.
8. B. Brickstad, B.L. Josefson, A Parametric Study of Residual Stresses in Multi-Pass Butt-Welded Stainless Steel Pipes, International Journalof Pressure Vessels and Piping 75, 1998, p. 11-25.B.
9. Brickstad, B.L. Josefson, A Parametric Study of Residual Stresses in Multi-Pass Butt-Welded Stainless Steel Pipes, International Journal of Pressure Vessels and Piping 75, 1998, p. 11-25.
10. Teng, T.L.; Lin C.C.: “Effect of Welding Conditions an Residual Stresses due to Butt Welds”, International Journal of Pressure Vessels and Piping , (1998) 857-864.

11. Wu, A.; Syngellakis, S.; Mellor, B.G.: "Finite Element Analysis of Residual Stresses in a Butt Weld", The Post Graduate Conference in Engineering Materials Proceedings, University of Southampton, England, (2001).
12. Chang, P.H., Teng, T.L., 2004. Numerical and experimental investigations on the residual stresses of the butt-welded, joints. *Comp. Mater. Sci.* 29, 511 – 522.
13. Aloraier, A.S. & Joshi, S. 2012. Residual stresses in flux cored arc welding process in bead-on-plate specimens. *Materials Science and Engineering*, A(534):13-21.
14. Bate, K.R. & Charles, R. & Warren, A. 2009. Finite element analysis of a single bead-on-plate specimen using SYS-WELD. *International Journal of Pressure Vessels and Pip-ing* 86:73-78.
15. Camilleri, D. & McPherson, N. & Gray, T. 2013. The applicability of using low transformation temperature welding wire to minimize unwanted residual stresses and distortions. *Int. J. Press. Vessel Piping*. 110:2-8.
16. Dizaji S A, Darendeliler H, Kaftanoğlu B, 2014 Effect of hardening models on different ductile fracture criteria in sheet metal forming *Int. J. Mat. Forming*, doi: 10.1007/s12289-014-1188-5.
17. John M. Chalmers; Peter Griffiths, eds. (2006). *Handbook of Vibrational Spectroscopy* (5 Volume Set). New York: Wiley.